

^{23}Na nuclear spin-lattice relaxation studies of $\text{Na}_2\text{Ni}_2\text{TeO}_6$

Y. Itoh¹

¹*Department of Physics, Graduate School of Science, Kyoto Sangyo University,
Kamigamo-Motoyama, Kita-ku Kyoto 603-8555, Japan*

(Dated: March 2, 2024)

We report on ^{23}Na NMR studies of a honeycomb lattice antiferromagnet $\text{Na}_2\text{Ni}_2\text{TeO}_6$ by ^{23}Na nuclear spin-echo techniques. The ^{23}Na nuclear spin-lattice relaxation rate $1/^{23}T_1$ exhibits critical divergence near a Néel temperature $T_N = 26$ K, a narrow critical region, and a critical exponent $w = 0.34$ in $1/^{23}T_1 \propto (T/T_N - 1)^{-w}$ for $\text{Na}_2\text{Ni}_2\text{TeO}_6$, and $T_N = 18$ K for $\text{Na}_2(\text{Ni}_{0.5}\text{Cu}_{0.5})_2\text{TeO}_6$. Although the uniform magnetic susceptibility of $\text{Na}_2\text{Ni}_2\text{TeO}_6$ exhibits a broad maximum at 35 K characteristic of low dimensional spin systems, the NMR results indicate three dimensional critical phenomenon around the Néel temperature.

PACS numbers:

I. INTRODUCTION

$\text{Na}_2\text{Ni}_2\text{TeO}_6$ is a quasi-two dimensional honeycomb lattice antiferromagnet [1–3]. The crystal structure of $\text{Na}_2\text{Ni}_2\text{TeO}_6$ consists of the stacking of Na and (Ni/Te) O_6 layers ($P6_3/mcm$) [2, 3]. The Néel temperature of $T_N \approx 27$ K was estimated from measurements of specific heat and the derivative of uniform magnetic susceptibility [3]. The magnetic susceptibility takes a broad maximum around 34 K [2, 3]. The Weiss temperature of $\theta = -32$ K and the superexchange interaction of $J/k_B = -45$ K were estimated from the analysis of Curie-Weiss law fit and a high temperature series expansion [3]. Although the Ni^{2+} ion must carry a local moment of $S = 1$ on the honeycomb lattice, the large effective moment $\mu_{\text{eff}} = 3.446\mu_B$ could not be explained by spin $S = 1$ with a g -factor of $g = 2$ [3]. The g -factor must be larger than 2 [2], or a Ni^{3+} ion and the intermediate state might be realized because of the tunable valence of Te^{4+} and Te^{6+} [3].

Spin frustration effects on a honeycomb lattice have renewed our interests, since the discovery of a possible spin liquid state in a spin-3/2 antiferromagnet [4]. Various magnetic ground states are competitive with each other on the honeycomb lattice [5].

In this paper, we report on ^{23}Na NMR studies of $\text{Na}_2\text{Ni}_2\text{TeO}_6$ and $\text{Na}_2(\text{Ni}_{0.5}\text{Cu}_{0.5})_2\text{TeO}_6$ polycrystalline samples. $\text{Na}_2(\text{Ni}_{0.5}\text{Cu}_{0.5})_2\text{TeO}_6$ still belongs to the same space group $P6_3/mcm$ as $\text{Na}_2\text{Ni}_2\text{TeO}_6$ [2, 6]. For the Cu substitution, we expected a possible enhancement of quantum effects from $S = 1$ to $1/2$. Since the solubility limit in the honeycomb lattice $\text{Na}_2(\text{Ni}_{1-x}\text{Cu}_x)_2\text{TeO}_6$ is about $x = 0.6$ [6], we selected the half Cu-substituted sample being away from the phase boundary. We observed three dimensional critical phenomenon in the ^{23}Na nuclear spin-lattice relaxation rate $1/^{23}T_1$ near $T_N = 26$ K for $\text{Na}_2\text{Ni}_2\text{TeO}_6$ and $T_N = 18$ K for $\text{Na}_2(\text{Ni}_{0.5}\text{Cu}_{0.5})_2\text{TeO}_6$. The broad maximum of uniform magnetic susceptibility is not the onset of magnetic long range ordering. In the antiferromagnetic state

of $\text{Na}_2\text{Ni}_2\text{TeO}_6$, we observed $1/^{23}T_1 \propto T^3$ which indicates conventional spin-wave scattering.

II. EXPERIMENTS

Powder samples of $\text{Na}_2\text{Ni}_2\text{TeO}_6$ have been synthesized by a conventional solid-state reaction method. Appropriate amounts of NiO, TeO_6 and Na_2CO_3 were mixed, palletized and fired a few times at 800 - 860°C and finally at 900°C for 24 hours in air. The products were confirmed to be in a single phase from measurements of powder X-ray diffraction patterns. Magnetic susceptibility χ at 1.0 T was measured by a superconducting quantum interference device (SQUID) magnetometer. Powder samples of $\text{Na}_2(\text{Ni}_{0.5}\text{Cu}_{0.5})_2\text{TeO}_6$ were previously synthesized and characterized [6].

A phase-coherent-type pulsed spectrometer was utilized to perform the ^{23}Na NMR (nuclear spin $I = 3/2$) experiments in an external magnetic field of 7.4847 T. The NMR frequency spectra were obtained from Fourier

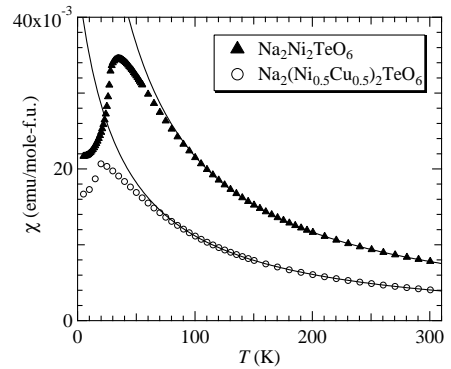


FIG. 1: Uniform magnetic susceptibility χ of $\text{Na}_2\text{Ni}_2\text{TeO}_6$ and $\text{Na}_2(\text{Ni}_{0.5}\text{Cu}_{0.5})_2\text{TeO}_6$. Solid curves are the results from least squares fits by a Curie-Weiss law.

transformation of the ^{23}Na nuclear spin-echoes. The ^{23}Na nuclear spin-lattice relaxation curves $^{23}p(t) = 1 - E(t)/E(\infty)$ (recovery curves) were obtained by an inversion recovery technique as a function of time t after an inversion pulse, where the nuclear spin-echoes $E(t)$, $E(\infty)[\equiv E(10T_1)]$ and t were recorded.

III. EXPERIMENTAL RESULTS AND DISCUSSIONS

A. Uniform magnetic susceptibility

Figure 1 shows uniform magnetic susceptibility χ of $\text{Na}_2\text{Ni}_2\text{TeO}_6$ and $\text{Na}_2(\text{Ni}_{0.5}\text{Cu}_{0.5})_2\text{TeO}_6$. The solid curves are the results from least squares fits by a Curie-Weiss law. We estimated the Weiss temperature $\theta = -27$ K and the effective moment $\mu_{\text{eff}} = 3.4\mu_{\text{B}}$ for $\text{Na}_2\text{Ni}_2\text{TeO}_6$, which agree with the previous report [3], and $\theta = -35$ K and $\mu_{\text{eff}} = 2.5\mu_{\text{B}}$ for $\text{Na}_2(\text{Ni}_{0.5}\text{Cu}_{0.5})_2\text{TeO}_6$. If the g -factor is $g = 2$, then $S = 1$ and $S = 1/2$ lead to $\mu_{\text{eff}} = 2.83\mu_{\text{B}}$ and $1.73\mu_{\text{B}}$, respectively. χ deviates below about 100 K from the Curie-Weiss law and takes a broad maximum at 35 K in $\text{Na}_2\text{Ni}_2\text{TeO}_6$. χ drops below about 20 K in $\text{Na}_2(\text{Ni}_{0.5}\text{Cu}_{0.5})_2\text{TeO}_6$.

B. NMR spectrum and recovery curves

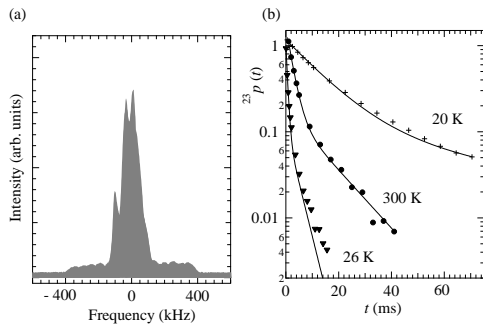


FIG. 2: (a) Fourier-transformed ^{23}Na NMR spectrum at 84.670 MHz and at 300 K. (b) ^{23}Na nuclear spin-lattice relaxation curves $^{23}p(t)$ at a central frequency. Solid curves are the results from least squares fits by eq. (1).

Figure 2(a) shows the Fourier-transformed spectrum of ^{23}Na spin-echoes at a Larmor frequency of 84.670 MHz and at 300 K. The central transition line of $I_z = 1/2 \leftrightarrow -1/2$ is affected by a nuclear quadrupole interaction [7]. The linewidth is about 150 kHz. The precise value of the Knight shift could not be determined within the present studies.

Figure 2(b) shows the recovery curves $^{23}p(t)$ with varying temperature. The solid curves are the results from

least-squares fits by a theoretical multi-exponential function for a central transition line ($I_z = 1/2 \leftrightarrow -1/2$)

$$^{23}p(t) = p(0)\{0.1e^{-t/^{23}T_1} + 0.9e^{-6t/^{23}T_1}\}, \quad (1)$$

where $p(0)$ and a ^{23}Na nuclear spin-lattice relaxation time $^{23}T_1$ are fit parameters. The theoretical function of eq. (1) well reproduces the experimental recovery data. Thus, the assignment of the exciting spectrum to the central transition line is justified *a posteriori*, too.

C. $\text{Na}_2\text{Ni}_2\text{TeO}_6$

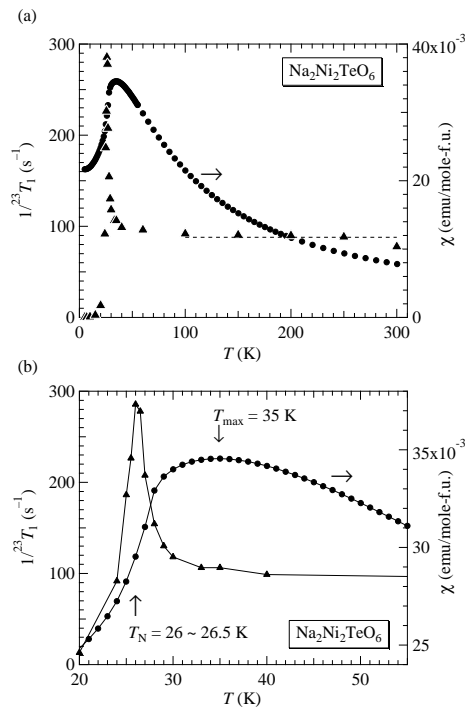


FIG. 3: (a) $1/^{23}T_1$ and uniform magnetic susceptibility χ against temperature. $1/^{23}T_1$ shows a critical divergence near $T_N = 26 \sim 26.5$ K and levels off above about 100 K. The broken line indicates $1/^{23}T_{1\infty} = 88 \text{ s}^{-1}$. (b) $1/^{23}T_1$ and χ against temperature in enlarged scales. Solid curves are visual guides.

Figures 3(a) and (b) show $1/^{23}T_1$ and uniform magnetic susceptibility χ against temperature. $1/^{23}T_1$ takes $1/^{23}T_{1\infty} = 88 \text{ s}^{-1}$ above about 100 K and shows a divergence at $26 \sim 26.5$ K which can be assigned to the Néel temperature T_N . Thus, the broad maximum of the magnetic susceptibility χ at 35 K is not due to the antiferromagnetic long range ordering but due to a low dimensional short range correlation developing on the honeycomb lattice antiferromagnets [8]. The result is consistent with the specific heat measurements [3].

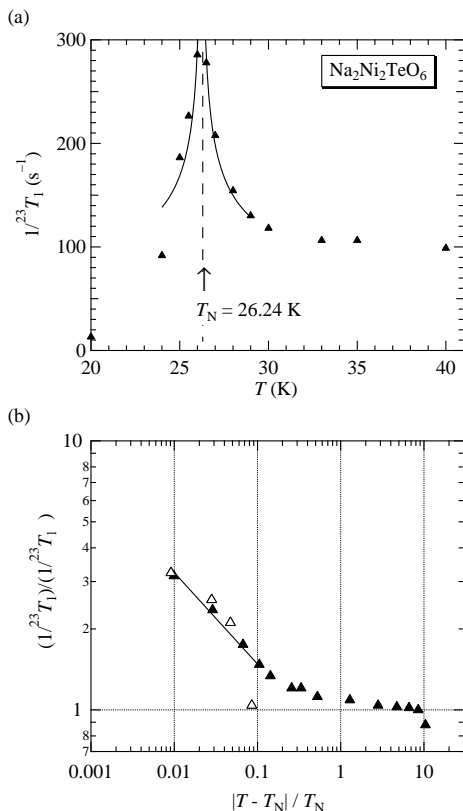


FIG. 4: (a) $1/^{23}T_1$ against temperature. The solid curve is the result from a least squares fit by eq. (2). The Néel temperature and the critical exponent were estimated to be $T_N = 26.24$ K and $w = 0.34$, respectively. (b) Log-log plots of normalized $(1/^{23}T_1)/(1/^{23}T_{1\infty})$ against reduced temperature $|T - T_N|/T_N$. Closed and open triangles are $1/^{23}T_1$ above and below T_N , respectively. The solid line indicates the result from a least squares fit by eq. (2).

Figure 4(a) shows $1/^{23}T_1$ against temperature and the result (the solid curve) from a least-squares fit by

$$\frac{1}{^{23}T_1} = \frac{C}{^{23}T_{1\infty}} \frac{1}{|T/T_N - 1|^w}, \quad (2)$$

where a constant C , a Néel temperature T_N , and a critical exponent w are fit parameters. The fitting results were $T_N = 26.24$ K and $w = 0.34$.

A mean field theory for a three dimensional isotropic Heisenberg antiferromagnet gives $w = 1/2$ [9]. A dynamic scaling theory gives $w = 1/3$ for a three dimensional isotropic Heisenberg model [10] and $w = 2/3$ for a three dimensional uniaxial anisotropic Heisenberg model [11]. The exponent of $w = 0.34$ indicates that $\text{Na}_2\text{Ni}_2\text{TeO}_6$ in the critical region is described by a three dimensional dynamical spin susceptibility. In passing, CuO exhibits a similar $w = 0.33$, a broad maximum in χ at 540 K, and $T_N = 230$ K [12].

Figure 4(b) shows log-log plots of normalized $(1/^{23}T_1)/(1/^{23}T_{1\infty})$ against reduced temperature

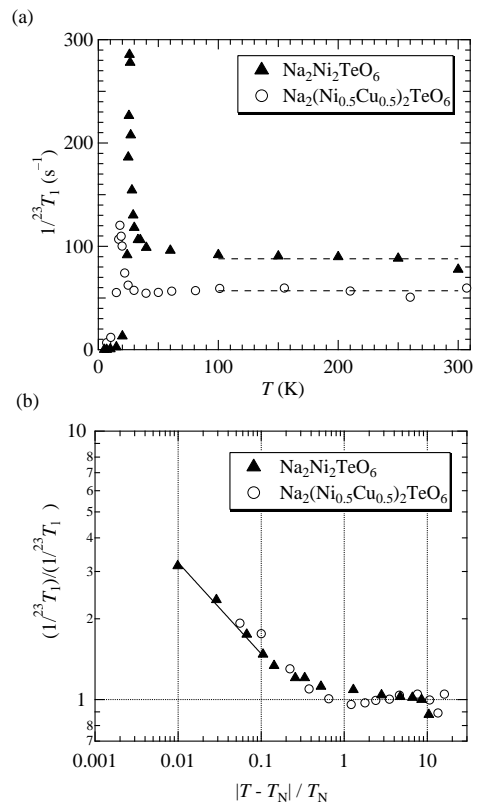


FIG. 5: (a) $1/^{23}T_1$ against temperature for $\text{Na}_2\text{Ni}_2\text{TeO}_6$ and $\text{Na}_2(\text{Ni}_{0.5}\text{Cu}_{0.5})_2\text{TeO}_6$. The broken lines indicate $1/^{23}T_{1\infty} = 88$ and 57 s^{-1} . (b) Log-log plots of normalized $(1/^{23}T_1)/(1/^{23}T_{1\infty})$ against reduced temperature $|T - T_N|/T_N$ for $\text{Na}_2\text{Ni}_2\text{TeO}_6$ ($T_N = 26.24$ K) and $\text{Na}_2(\text{Ni}_{0.5}\text{Cu}_{0.5})_2\text{TeO}_6$ ($T_N = 18$ K). The solid line is eq. (2) with the critical exponent of $w = 0.34$.

$|T - T_N|/T_N$. The solid line indicates the result from a least squares fit by eq. (2).

The onset of increase in the NMR relaxation rate near T_N empirically categorizes critical regions. The region of $|T - T_N|/T_N \leq 10$ has been assigned to the renormalized classical regime with a divergent magnetic correlation length toward $T = 0$ K [13]. The region of $|T - T_N|/T_N \leq 1.0$ has been assigned to the three dimensional critical regime with a divergent magnetic correlation length toward T_N . Thus, the narrow critical region of $|T - T_N|/T_N \leq 1$ also empirically categorizes $\text{Na}_2\text{Ni}_2\text{TeO}_6$ to the three dimensional critical regime.

At high temperatures of $T \gg J$, the spin system is in the exchange narrowing limit. Then, $1/^{23}T_1$ is expressed by

$$\frac{1}{^{23}T_{1\infty}} = \sqrt{2\pi} \frac{S(S+1)}{3} \frac{z_n (\gamma_n A)^2}{\omega_{ex}}, \quad (3)$$

$$\omega_{ex}^2 = \frac{2}{3} S(S+1) z \left(\frac{J}{\hbar} \right)^2, \quad (4)$$

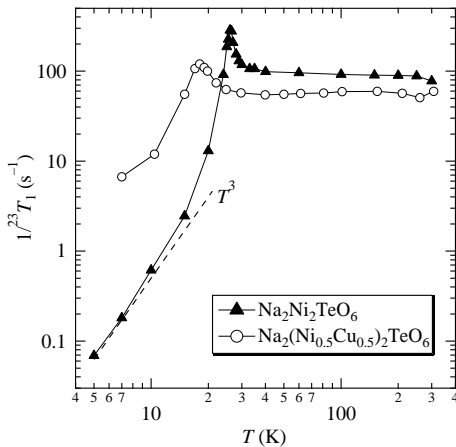


FIG. 6: Log-log plots of $1/^{23}T_1$ against temperature for $\text{Na}_2\text{Ni}_2\text{TeO}_6$ and $\text{Na}_2(\text{Ni}_{0.5}\text{Cu}_{0.5})_2\text{TeO}_6$. A broken line indicates a function of eq. (5). Solid curves are visual guides.

where $^{23}\gamma_n/2\pi = 11.262 \text{ MHz/T}$ is the ^{23}Na nuclear gyromagnetic ratio, A is a hyperfine coupling constant, and ω_{ex} is an exchange frequency [14]. z_n is the number of Ni ions nearby a ^{23}Na nuclear. z is the number of the nearest neighbor Ni ions. Assuming $J = 45 \text{ K}$, [3] $S = 1$, and $z = 3$, we obtained $\omega_{ex} = 12 \times 10^{12} \text{ s}^{-1}$. From eq. (3) with $1/^{23}T_{1\infty} = 88 \text{ s}^{-1}$, we derived the hyperfine coupling constant $A = 2.0 \text{ kOe}/\mu_B$, which is nearly the same as that of $\text{Na}_3\text{Cu}_2\text{SbO}_6$ [15].

D. $\text{Na}_2(\text{Ni}_{0.5}\text{Cu}_{0.5})_2\text{TeO}_6$

Figure 5(a) shows $1/^{23}T_1$ against temperature for $\text{Na}_2\text{Ni}_2\text{TeO}_6$ and $\text{Na}_2(\text{Ni}_{0.5}\text{Cu}_{0.5})_2\text{TeO}_6$. For the half substitution of Cu for Ni, $1/^{23}T_{1\infty}$ and T_N decrease to 57 s^{-1} and 18 K , respectively. Extrapolating linearly T_N with $\Delta T_N = -8 \text{ K}$ per half Cu to full Cu substitution, one may infer $T_N = 10 \text{ K}$ of a hypothetical spin-1/2 honeycomb lattice $\text{Na}_2\text{Cu}_2\text{TeO}_6$,” although actual $\text{Na}_2\text{Cu}_2\text{TeO}_6$ is known to be monoclinic and an alternating spin chain system [16, 17].

Figure 5(b) shows log-log plots of normalized $(1/^{23}T_1)/(1/^{23}T_{1\infty})$ against reduced temperature $|T - T_N|/T_N$ for $\text{Na}_2\text{Ni}_2\text{TeO}_6$ ($T_N = 26.24 \text{ K}$) and $\text{Na}_2(\text{Ni}_{0.5}\text{Cu}_{0.5})_2\text{TeO}_6$ ($T_N = 18 \text{ K}$). The solid line indicates eq. (2) with the critical exponent of $w =$

0.34. The critical region of $\text{Na}_2(\text{Ni}_{0.5}\text{Cu}_{0.5})_2\text{TeO}_6$ is still narrow as the same as that of $\text{Na}_2\text{Ni}_2\text{TeO}_6$. Simply, T_N decreases. No dimensional crossover is observed.

E. Below T_N

Figure 6 shows log-log plots of $1/^{23}T_1$ against temperature for $\text{Na}_2\text{Ni}_2\text{TeO}_6$ and $\text{Na}_2(\text{Ni}_{0.5}\text{Cu}_{0.5})_2\text{TeO}_6$. With cooling down below T_N , $1/^{23}T_1$ rapidly decreases. The broken line indicates a T^3 function as a visual guide. In conventional antiferromagnetic states, the nuclear spin transitions are caused by Raman scattering and three magnon scattering [18]. Then, $1/T_1$ is expressed by

$$\frac{1}{T_1} \propto \left(\frac{T}{T_N}\right)^3 \quad (5)$$

in a temperature range of $T_N > T \gg T_{AE}$, where T_{AE} corresponds to an energy gap in the spin wave spectrum [18]. The energy gap is due to a crystalline anisotropy field. The rapid drop of $1/^{23}T_1$ below T_N results from the suppression of low energy excitations by the energy gap. Below T_{AE} , an activation-type temperature dependence should be observed in $1/T_1$. Since no activation behavior was observed down to 5 K , one may estimate $T_{AE} < 5 \text{ K}$.

IV. CONCLUSIONS

In conclusion, we found three dimensional critical phenomenon near $T_N = 26 \text{ K}$ for $\text{Na}_2\text{Ni}_2\text{TeO}_6$ and $T_N = 18 \text{ K}$ for $\text{Na}_2(\text{Ni}_{0.5}\text{Cu}_{0.5})_2\text{TeO}_6$ from measurements of the ^{23}Na nuclear spin-lattice relaxation rate $1/^{23}T_1$. We have analyzed the NMR results by Ni^{2+} with $S = 1$ and obtained sound values of parameters for $\text{Na}_2\text{Ni}_2\text{TeO}_6$. We attribute the deviation from the Curie-Weiss law and the broad maximum of uniform magnetic susceptibility to two dimensional spin-spin correlation on a honeycomb lattice.

The author thanks M. Isobe (Max Planck Institute) for X-ray diffraction measurements, K. Morimoto, C. Michioka, K. Yoshimura (Kyoto University) for sample preparation and characterization at an early stage.

V. REFERENCES

-
- [1] Y. Miura, R. Hirai, Y. Kobayashi and M. Sato: J. Phys. Soc. Jpn. **75** (2006) 084707.
 - [2] R. Berthelot, W. Schmidt, A. W. Sleight and M. A. Subramanian: J. Solid State Chem. **196** (2012) 225.
 - [3] R. Sankar, I. P. Muthuselvam, G. J. Shu, W. T. Chen, S. K. Karna, R. Jayavel and F. C. Chou: CrystEngComm. **16** (2014) 10791.
 - [4] O. Smirnova, M. Azuma, N. Kumada, Y. Kusano, M. Matsuda, Y. Shimakawa, T. Takei, Y. Yonesaki and N. Kinomura: J. Am. Chem. Soc. **131** (2009) 8313.
 - [5] J. B. Fouet, P. Sindzingre and C. Lhuillier: Eur. Phys. J. B **20** (2001) 241.

- [6] K. Morimoto, Y. Itoh, C. Michioka, M. Kato and K. Yoshimura: J. Magn. Magn. Mater. **310** (2007) 1254. $\text{Na}_2(\text{Ni}_{1-x}\text{Cu}_x)_2\text{TeO}_6$ with $0 \leq x \leq 0.60$ belongs to the space group $P6_3/mcm$, while $\text{Na}_2(\text{Cu}_{1-x}\text{Ni}_x)_2\text{TeO}_6$ with $0 \leq x \leq 0.05$ belongs to the space group $C2/m$ (unpublished works).
- [7] A. Abragam, *Principles of Nuclear Magnetism*, Oxford University Press, Oxford (1961).
- [8] N. Onishi, K. Oka, M. Azuma, Y. Shimakawa, Y. Motome, T. Taniguchi, M. Hiraishi, M. Miyazaki, T. Masuda, A. Koda, K. M. Kojima and R. Kadono: Phys. Rev. B **85** (2012) 184412.
- [9] T. Moriya: Prog. Theor. Phys. **28** (1962) 371.
- [10] B. I. Halperin and P. C. Hohenberg: Phys. Rev. Lett. **19** (1967) 700.
- [11] E. Riedel and F. Wegner: Phys. Rev. Lett. **24** (1970) 730.
- [12] Y. Itoh, T. Imai, T. Shimizu, T. Tsuda, H. Yasuoka and Y. Ueda: J. Phys. Soc. Jpn. **59** (1990) 1143.
- [13] Y. Itoh, C. Michioka, K. Yoshimura, K. Nakaajima and H. Sato: J. Phys. Soc. Jpn. **78** (2009) 023705.
- [14] T. Moriya: Prog. Theor. Phys. **16** (1956) 641.
- [15] C. N. Kuo, T. S. Jian and C. S. Lue: J. Alloys Com. **531** (2012) 1.
- [16] J. Xu, A. Assoud, N. Soheilnia, S. Derakhshan, H. L. Cuthbert, J. E. Greedan, M. H. Whangbo and H. Kleinke: Inorg. Chem. **44** (2005) 5042.
- [17] K. Morimoto, Y. Itoh, K. Yoshimura, M. Kato and K. Hirota: J. Phys. Soc. Jpn. **75** (2006) 083709.
- [18] D. Beeman and P. Pincus: Phys. Rev. **166** (1968) 359.